WCTE 2018
2018 World Conference on Timber Engineering
August 20 - 23, 2018 | Seoul, Republic of Korea

Simulating failure mechanisms in wooden boards with knots by means of a microstructure-based multisurface failure criterion

Markus Lukacevic[1], Josef Füssl[1], Josef Eberhardsteiner[1]

ABSTRACT: As a natural composite, the failure behavior of wood highly depends on structural features on several lower length scales. Thus, an approach for the prediction of failure mechanisms of wood has been proposed, leading to a better description of mechanical processes in wood and, thus, to an improved performance of wood-based products in service.

In the several steps of our damage concept for clear-wood [1, 2, 3], first, failure criteria for the two main wood cell types, namely early- and latewood, were obtained by an extensive investigation of load combinations on unit cells. These were then applied in the next step to simulations of a clear-wood unit cell, which allowed the identification and classification of the main failure mechanisms at the clear-wood level. Based on these findings, a single multisurface failure criterion was formulated, which is able to represent brittle and ductile failure mechanisms. Furthermore, to enable the simultaneous simulation of plastic failure and crack initiation, an algorithm for multisurface failure criteria was presented.

This new failure criterion was implemented into previous developments of a numerical simulation tool for wooden boards [4, 5, 6, 7], which enables the mathematical description of fiber deviations in the vicinity of virtually reconstructed knots. Thus, realistic simulations of complex failure mechanisms of wooden boards with knots will be rendered possible. That way, the simulation tool can be used in the development of new wood composites, by making the material wood more predictable and, thus, more interesting for engineering applications.

KEYWORDS: knots, failure mechanisms, material modeling, multisurface failure criteria, XFEM

1 INTRODUCTION

Wood is one of the oldest and, at the same time, one of the most complex building materials. However, just in recent years wood has been rediscovered as a material combining economic sustainability and an excellent mechanical performance, and thus, has been used for increasingly complex constructions. For structural purposes, defect free wood (also called clear-wood) is the possibly best building material produced by nature with respect to strength-to-weight and stiffness-to-weight characteristics. However, due to the natural growth process of trees, wooden boards, typically used for structural load bearing elements, show a high amount of random fluctuation in their mechanical properties [8, 9]. In particular, knots frequently lead to failure of timber structures [10]. Current design codes are based on the assumption of homogeneous wooden boards and property fluctuations due to inhomogeneities are taken into account by safety factors, which can lead to conservative or unsatisfactory structural designs [11, 12, 13]. For this reason, exploiting the full potential of wood still poses a challenging task to structural engineers, which represents a major disadvantage compared to competing materials.

In [14] a framework for sensitivity analysis and robust design optimization of glued laminated timber structures was presented, which is based on a random material model for both stiffness and strength properties of individual laminations. There a closed solution for determining stiffness and strength profiles from laser scan data of wooden boards was incorporated into the framework. Based on this data obtained through laser scanning, a procedure already incorporated in numerous industrial manufacturing sites, the 3D knot geometry is reconstructed automatically [15]. Subsequently, a 3D finite element model is used to determine the effective stiffness of each knot group [4, 5, 6]. For the same knot groups, the effective strength values are estimated using indicating properties (IP) [16]. From the calculated set of values, a so-called stiffness and strength profile can be determined for each board. But this method for obtaining effective strength values for knot sections with IPs inherently limits the quality of the resulting strength profiles and, thus, also of the mechanical model of structural timber elements in further design optimization processes. Therefore, our goal is to simulate failure

[1] Markus Lukacevic, Vienna University of Technology, markus.lukacevic@tuwien.ac.at
Josef Füssl, Vienna University of Technology, josef.fuessl@tuwien.ac.at
Josef Eberhardsteiner, Vienna University of Technology, josef.eberhardsteiner@tuwien.ac.at

mechanisms in wooden elements as realistically as possible. Such a simulation tool, which is able to also consider knots and fiber deviations in their vicinities, can then be used on one hand to obtain better effective strength properties, which are used for the generation of random process models, and on the other hand during the product development process of new engineered wood products or new types of wood composites, where the base product is often a simple wooden board.

In the next section, Section 2, the multiscale modeling approach, which enables the realistic modeling of clear-wood fracture mechanisms, is revisited. The application of the obtained multisurface failure criterion is then presented in Section 3 for two examples, showing the approach's capability of predicting failure mechanisms of clear-wood for common timber engineering problems. In Section 4, the failure criterion is then implemented into a previously developed numerical simulation tool, which allows the future simulation of failure processes in wooden boards with knots. Finally, in Section 5 concluding remarks and an outlook to future developments are given.

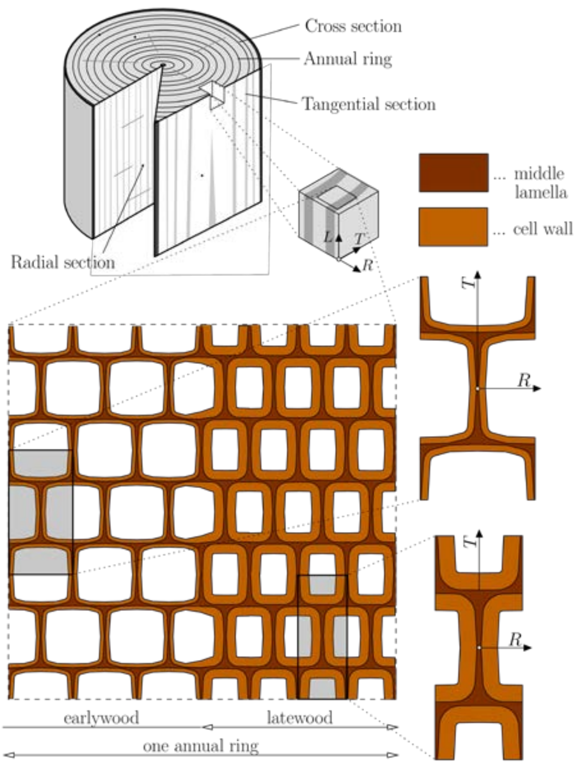

Figure 1: *Multiscale modeling approach for the determination of global crack direction and initiation [2]*

2 MULTISCALE MODELING APPROACH TO DESCRIBE FAILURE OF WOOD

Due to the complex microstructure of wood, traditional strength prediction methods are usually not able to capture mechanisms, close to or after the point of failure, correctly. By applying new approaches, based on detailed material models on lower length scales, effects, like stress redistributions caused by localized cell wall failure, can be considered within numerical simulations.

Such an approach was proposed in [1, 2] (see Figure 1), where, first, failure mechanisms of the two main clear-wood layers, late- and earlywood, were identified at the wood cell level by using a unit cell approach in combination with the XFEM. The results from an extensive range of loading combinations enabled a classification of the obtained failure mechanisms and, in a next step, the determination of failure surfaces for each failure mode, to which a corresponding global crack direction was assigned to.

In a next homogenization step [3], the two new multisurface failure criteria were applied to a new unit cell at the annual year ring level, where the layered structure of late- and earlywood was modeled individually. Another extensive parameter study on loading conditions led to the identification and classification of the main failure mechanisms at the clear-wood level. Finally, the results on this length scale were used to obtain a single multisurface failure criterion for clear-wood (see Figures 2 and 3), where XFEM is used to describe brittle failure mechanisms under tensile and shear loading, and plastic behavior to describe plastification-like failure mechanisms under compression.

This multiscale modeling approach allows the consideration of various wood-specific failure mechanisms with a single multisurface failure criterion, which is solely based on simulation results at lower length scales. For this reason, all strength parameters are determined physically meaningful and no empirical assumptions are necessary.

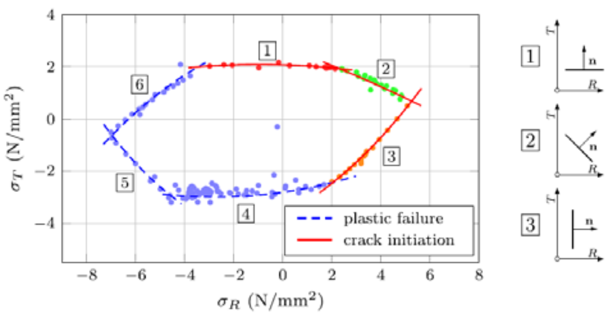

Figure 2: *Failure surfaces for the annual ring unit cell in the* $\boldsymbol{\sigma_R}$*-*$\boldsymbol{\sigma_T}$ *plane, with blue surfaces identifying ductile and red ones brittle failure mechanisms, and for latter ones assigned crack directions after crack initiation are [3]*

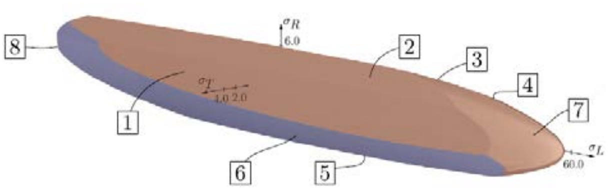

Figure 3: *3D representation of the failure surfaces in the* $\boldsymbol{\sigma_L}$*-*$\boldsymbol{\sigma_R}$*-*$\boldsymbol{\sigma_T}$ *stress space with the shear stresses being equal to zero* ($\boldsymbol{\tau_{LR}} = \boldsymbol{\tau_{LT}} = \boldsymbol{\tau_{RT}} = 0$) *[3]*

3 APPLICATION TO CLEAR-WOOD

The comparison of the new failure criterion to a large set of experiments of clear-wood spruce samples in the LR-plane showed that both ductile and brittle failure mechanisms could be predicted very well [3]. Next, we show the application of the failure criterion to a common timber-engineering example and its capability also to correctly predict the post-peak behavior in a typical three-point bending test.

3.1 Dowel-type timber connection

For the application of the multisurface failure criterion to a timber-engineering example, the embedment behavior of a single-dowel connection test [17] was simulated. Further details on material and simulation properties are described in [3]. For this so-called full-hole test, a wood sample is fixed at the bottom and two steel plates move vertically downwards, applying a load to the embedded dowel (see Figure 4(a)).

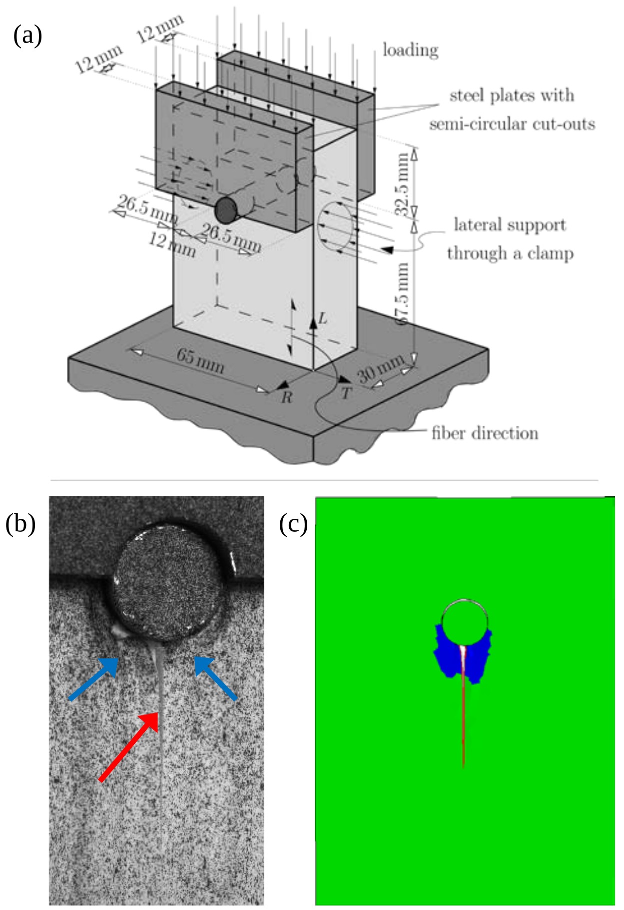

Figure 4: *(a) Experimental setup for a dowel-type connection test and comparison of (b) the experimental result, where the red arrow marks the propagating crack and the blue one the densification of wood material due to embedment pressure, and (c) the simulation results with plastified regions (blue) and the developed crack underneath the dowel (red) [3]*

Figure 4(b) shows a close-up of the experimental test. As the dowel moves downwards, the wood specimen is exposed to corresponding embedment pressure. This leads to compressive stress in vertical and, thus, longitudinal material direction, but also to perpendicular-to-grain tension. As the strength for the latter one is significantly lower, a vertical crack starts to form below the dowel. Then, almost simultaneously, the crack propagates in vertical direction (marked with red) and plastification-like effects, starting close to the dowel-wood contact region, can be observed. The latter effect can be noticed by a densification of the black and white spray speckle pattern, marked in blue. The same failure mechanisms can be reproduced very well by the developed model. In summary, it can be noted that the failure criterion is capable of representing both plastic failure mechanisms and the formation of cracks at the same time and in the same regions.

3.2 Evaluation of fracture energy for a three-point bending test

To validate the model's ability to predict load-displacement curves even after the load peak and, thus, its capability to realistically estimate the correct fracture energy for typical loading conditions of clear-wood, the multisurface failure criterion is applied to a three-point bending test example found in literature [18].
Figure 5 shows the experimental setup, which can be used to determine fracture energies with respect to the wood orientation (here for the two orientations TL and RL), and the corresponding finite element model with the used mesh. An initial notch ensures a stable crack extension until complete separation of both crack faces.

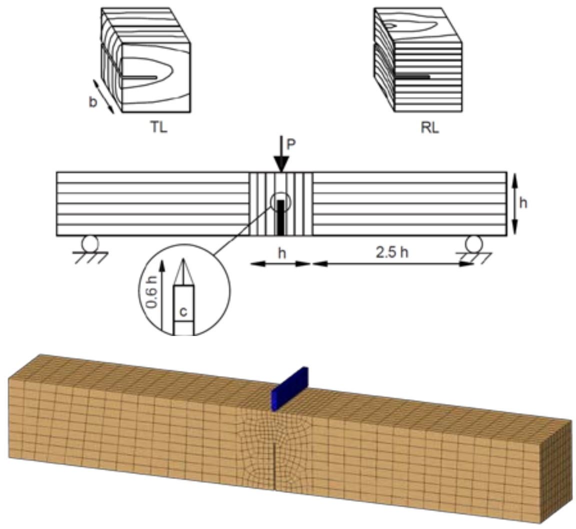

Figure 5: *(a) Experimental setup* [18] *and (b) FE model of the three-point bending test of a beam with an initial notch*

Figure 6 shows the comparison of experimentally (grey line, denoted with number one) and numerically (blue) obtained load-displacement curves for both configurations. Within the FE simulation, the first small drop in the load-displacement curve can be noticed at the first occurrence of cracks next to the center of the initial notch. The maximum load is then reached for both configurations when the entire first row of elements adjacent to the initial notch is cracked. Finally, a sequence of load drops follows until the simulation stops. It can be noticed that the load-displacement curve can be predicted very well by the numerical simulation. In addition, it must

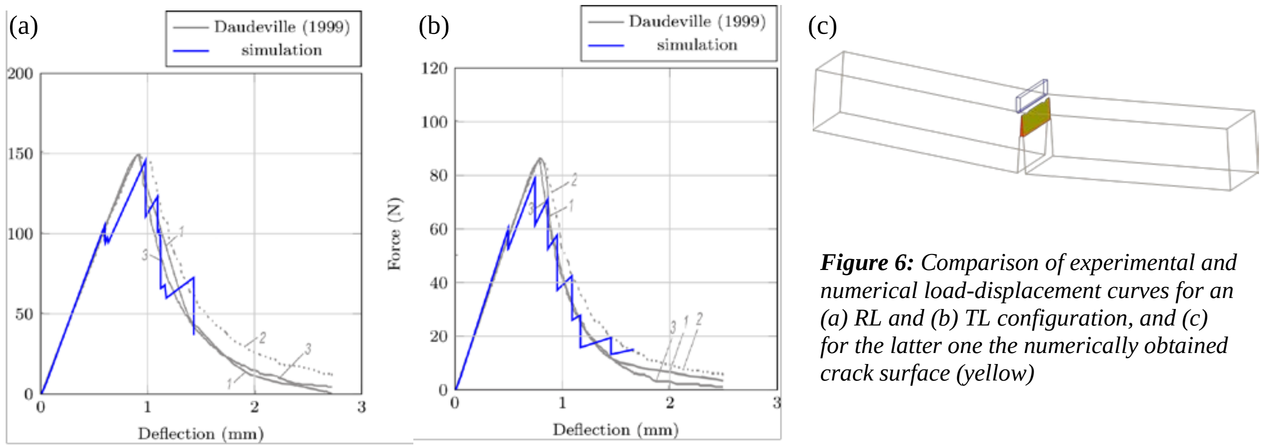

__Figure 6:__ Comparison of experimental and numerical load-displacement curves for an (a) RL and (b) TL configuration, and (c) for the latter one the numerically obtained crack surface (yellow)

be emphasized that the final crack surfaces, which can be seen in Figure 6(c) for the TL configuration and which also occurred in the experiment, are simply caused by the used multisurface failure criterion and no crack path was predefined.

4 IMPLEMENTATION INTO NUMERICAL SIMULATION TOOL FOR WOODEN BOARDS

By implementing this new failure criterion into previous developments of a numerical simulation tool for wooden boards [4-6], which is able to consider morphological features at the single board level, like virtually reconstructed knot inclusions and fiber deviations in their vicinities, realistic simulations of complex failure mechanisms of not only single wooden boards and their use in timber connections but also of more complex wood-based products, like Glulam and CLT elements, will be rendered possible. To be able to simulate failure mechanisms in wooden boards with knots, especially with a future implementation into automated processes in mind, several steps are necessary: knot geometries must be reconstructed based on easily available geometric data, fiber deviations in the vicinity of knots must be modelled realistically and various geometric and methodical issues, e.g. stemming from complex 3D crack surfaces, must be tackled adequately.

4.1 Knot morphology reconstruction

Within the numerical simulation tool, knots are modelled as rotationally symmetric cones. As the goal of our research is the realistic simulation of failure mechanisms of wooden boards with knots, we now have to virtually reconstruct the knot morphology. To ensure the future applicability of our approach to real wooden boards, our reconstruction algorithm relies on laser scan data that is obtained during the grading process of individual timber boards. Such laser scanning devices are already a widely used part of the wood processing chain to improve the yield of grading. By using the so-called tracheid effect, which describes the light propagation in wood [19, 20, 21], the fiber angles on the wooden board surfaces can be obtained. These values are then used to automatically determine knot areas on all four surfaces of the respective board. From the knot areas, the three-dimensional knot geometry is reconstructed employing an automated algorithm. A simulated-annealing optimization scheme is incorporated to identify most probable knot arrangements for cases were the available data leaves room for ambiguity. The different aspects of this reconstruction algorithm are discussed in detail in [15].

In the following, only the main features are summarized:

1) In a first step, knot areas are identified based on the superposition of the in-plane fiber angle and the out-of-plane fiber angle, which, for the present study, is obtained on basis of the empirical model proposed in [22]. By comparing the three-dimensional fiber angle estimate with a threshold value, it is possible to determine the individual knot areas. Subsequently, the knot areas are grouped to what is supposed to be the knot groups on basis of a deterministic criterion.
2) In addition, the pith location is estimated by fitting multiple circles to the year rings visible in photographs of cross sections at both ends of the board. The pith is represented by a linear curve connecting the arithmetic means of the center points at both ends.
3) Modelling each knot as a rotationally symmetric cone defined by a cone apex, a knot axis vector and an opening angle, in a next step the knot axis vectors are reconstructed based on an automated scheme. The reconstruction algorithm relies on the identified knot areas from step (1) and the location of the pith from step (2) and works for knot groups with an arbitrary number of knot areas. All pairs of knot areas that do not share the same face of the board, are connected by a knot axis candidate.
   For each knot axis candidate, a normalized measure is computed to indicate its goodness of fit. This measure is based on the normal distance between axis and pith and the distance between the two knot areas, the axis is associated with. Then, the axes are sorted by their fitness measure and an iterative selection process is started. In each iteration step, the axis with the best fitness measure is selected and removed from the pool of axis candidates. To ensure a certain quality of fit, the selected axis is compared with predefined critical values. This comparison includes the fitness measure itself and the inclination angle between axis and pith. In case the selected candidate does not comply with

the given criteria, the next iteration step is started. Since each knot area can only belong to one knot and, therefore, to one knot axis, all other candidates associated with one of the knot areas belonging to the selected axis are also removed from the candidate pool. This step is iterated as long as there are axis candidates in the pool.

In case of knot areas remaining, they are assumed to belong to knots that are only partly penetrating the board and, therefore, are associated with only one knot area. The knot axes of those knots are reconstructed based on a combination of an estimated inclination angle and the knot area position. For the inclination angle estimation, the average inclination angle of already reconstructed knot axes is used.

4) For each reconstructed knot axis, the cone opening angle is computed such that the cone surface fits the boundaries of the associated knot areas in the least-square sense.
5) To improve the reconstruction quality of this principally deterministic algorithm, a simulated-annealing optimization scheme [23] is employed which aims at minimizing the reconstruction error. As error measure, the difference between actual knot areas and knot areas from intersecting the reconstructed cones with the board is used. While the computational effort is high in comparison to the deterministic algorithm, for specific cases of knot configurations, a significantly better approximation can be obtained.

4.2 Fiber deviations in the vicinity of knots

The 3D knot geometries can now be used within 3D finite element analyses. Thus, after meshing of the geometry, the 3D fiber angle course is computed in each integration point as outlined in [6]. Following the so-called grain-flow analogy and using an algorithm, proposed by [24], the longitudinal-tangential fiber directions can be determined by mimicking the trajectories of a laminar fluid flowing along the x-axis, with knots as elliptical obstacles. The angle in radial-longitudinal direction, also known as the dive angle, is obtained from polynomials fitted to photographs of knot sections. Further developments of this approach, now, also allow for the combination of multiple close-by knots with intersecting fiber deviation regions, a configuration which often occurs in real wooden boards, where knots tend to appear in so-called knot clusters.

The clear-wood stiffness tensor itself is obtained from a micromechanical multiscale-model [25] with mass density and moisture content as main input factors. For the analysis, it is assumed that the clear-wood stiffness tensor remains the same within one board. In addition, the resulting stiffness tensor is used for the undisturbed and knot-free clear-wood sections within the board.

4.3 Cracks in the vicinity of knots

To solve the complex problem of discrete cracking close to interfaces of highly orthotropic bimaterials (interface between knot and surrounding clear-wood), new algorithms were developed and implemented into commercial FE software by means of so-called user subroutines. The current implementation of XFEM, which allows the modeling of discrete cracking, into the used commercial finite element software Abaqus, causes several limitations to the modeling of cracks in areas with highly varying material directions. Within the FE model, each element either can be cracked or not cracked, which means that cracks cannot stop inside of an element. In addition, only one crack per element is allowed. One consequence of these implementation limitations is that once a moving crack reaches a knot it cannot propagate further, because within our model it is assumed that the knot itself cannot fail. To visualize this problem and the resulting modeling repercussions, we examine the simple example of a wooden board with a single knot (see Figure 7). The board's length coincides with the global longitudinal direction and the pith location is above the board. Thus, the depicted knot faces towards the global radial direction and the fiber deviations in the vicinity of the knot depend almost exclusively on the before-mentioned second part of the fiber deviation algorithm, the fitted polynomials, due to the small thickness of the board. Therefore, on the left end of the board, the local longitudinal fiber direction is parallel to the pith. When we get closer to the knot, the fibers are deviated downwards, until in close proximity to the knot they are almost parallel to it and nearly perpendicular to the fiber direction outside the sphere of influence of the knot.

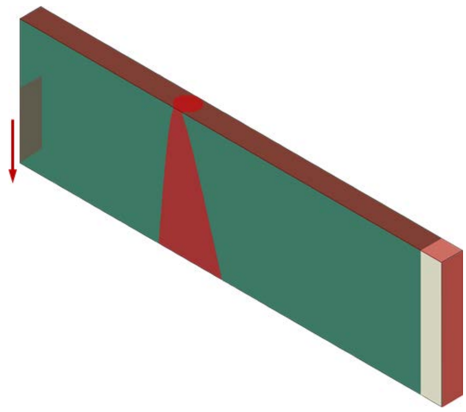

Figure 7: *Model of a wooden board with a single knot, where the top and right red surfaces indicate the fixed boundary conditions and the left red surface the applied vertical displacement boundary condition.*

As shown by the reddish surfaces in Figure 7, the board is fixed on the top and right narrow surfaces and the lower half of the left surface is subjected to a vertical displacement. If we now apply the original multisurface failure criterion to this example, this leads to the initiation of perpendicular-to-grain tensile failure directly above the applied boundary condition on the left (see Figure 8). Then the crack propagates following the fiber course until it reaches the interface between clear-wood and knot, where further cracking is made impossible due to the abovementioned restrictions. The corresponding time point on the load-displacement curve in Figure 9 is the local minimum of the blue dashed curve. It can be noticed that after this point the load increases significantly above the level of the original peak load value, which indicates that unrealistically high displacements can be applied after the crack has stopped at the interface. At the end of the simulation, the whole region below the first crack fails at the same time, which can also be noticed by the final drop in the corresponding curve.

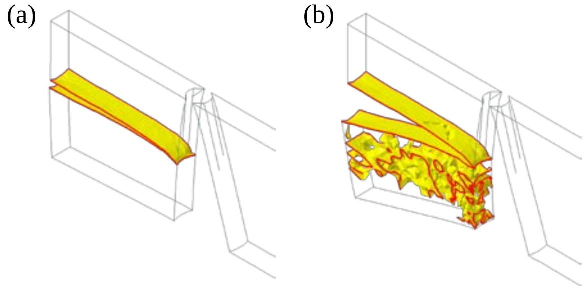

Figure 8: *Simulation result for the multisurface failure criterion without the interface algorithm, where at (a) the propagating crack reaches the clear-wood/knot interface and at (b) the simulation stops with multiple crack events occurring below the first crack*

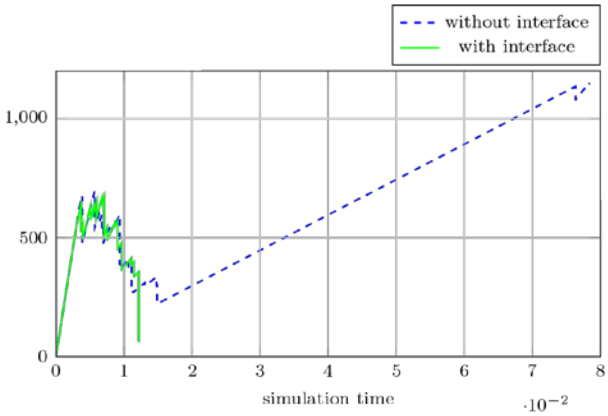

Figure 9: *Comparison of the reaction forces over the simulation time for the two model versions without and with the interface algorithm*

In order to prevent this obviously unrealistic failure behavior, we now introduce an algorithm, which controls the crack initiation criterion in close proximity to the knot. Figure 10 shows the idea behind this algorithm. For the illustrated finite element, a fictive clear-wood/knot interface below the element and approximately in the xz-plane is assumed. The normal vector on this interface is defined as $\boldsymbol{n}_{int}$ and shown in black in the figure. Now, we assume that an existing crack in the adjacent elements reaches the current element, creating a preexisting crack edge (blue). The normal vector $\boldsymbol{n}_{MSF}$ (red vector) on the new crack surface can then be obtained with the previously described multisurface failure criterion. If the corresponding new crack surface would now lie closer to the knot interface than the surface determined by $\boldsymbol{n}_{int}$, the crack initiation normal vector is overruled. I.e., as the black surface in Figure 10 is parallel to the knot interface, the red surface is not allowed to face towards the interface and, thus, a crack is not allowed to propagate towards a knot if the element lies within the defined interface region in close proximity to a knot.

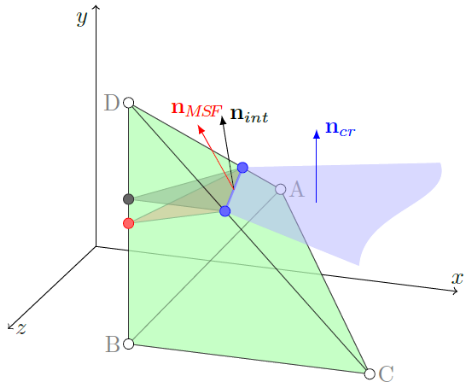

Figure 10: *Determination of crack normal vector in the vicinity of knots (red=normal vector from multisurface failure criterion, black=vector, normal to closest point on knot and blue=normal vector of existing crack in adjacent element).*

The necessity for this algorithm results from the fact that you cannot simply specify n_{int} as the crack initiation normal vector for all interface elements, otherwise you prevent a crack from ever leaving this interface region again. Thus, e.g., if for another boundary condition the crack had started on the bottom surface next to the knot, it would never leave the close proximity of the knot, although one would expect it to follow the fiber course away from the knot.

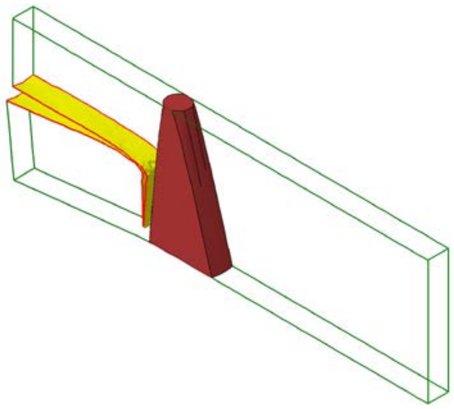

Figure 11: *Simulation result for the multisurface failure criterion with the interface algorithm, where at the propagating crack is deflected according to the longitudinal fiber direction before it reaches the clear-wood/knot interface*

The result of the simulation of the sample board, now with the algorithm for the interface region, is shown in Figure 11. In the beginning, the failure mechanism is the same as for the first simulation, but as soon as the propagating crack reaches the interface region, the algorithm causes the crack to deviate downwards. Thus, crack propagation is never interrupted and the simulation only stops closely before the crack would reach the bottom surface because an equilibrium can no longer be found. The corresponding force-displacement curve in Figure 9 (green) shows that the initial failure behavior is almost identical for both simulations, but in comparison to the first simulation, now the expected sharp decrease in force can be observed.

5 CONCLUSIONS AND OUTLOOK

An extension of our numerical simulation tool for wooden boards was presented. The basis for modeling realistic failure mechanisms in such boards is a previously developed multisurface failure criterion, which has been developed by investigating the failure behavior of clear-wood in an multiscale modeling approach at two lower length scales in extensive numerical simulations. Thus, all strength parameters were determined physically meaningful and no empirical assumptions were necessary. This failure criterion is now able to reproduce ductile as well as brittle failure mechanisms of clear-wood.

The application to an engineering example, a dowel-type connection, and to an often used three-point bending experiment, found in literature, showed that with this approach we are able not only to realistically predict failure mechanisms of clear-wood but also that the post-peak behavior and, thus, the typical fracture energies, can be modeled correctly.

Finally, to apply this failure criterion to wooden boards with knots, which are the main strength-reducing factor in most timber engineering applications, we revisited our algorithm for the automatic reconstruction of knot morphologies, which is based on data obtained from widely used laser scanning devices. In combination with a fiber deviation model, which is also able to describe the complex fiber directions in-between close-by knots, now, finite element simulations of knots sections are rendered possible. The simulation of discrete cracking in regions with highly varying material directions, i.e. in the vicinity of knots, causes several problems, which must be tackled carefully. The solution to such a problem, the unwanted ceasing of a crack process at a knot/clear-wood interface, was presented and shown on an example. This necessary adaption of the crack initiation algorithm, which has been implemented into the commercial FE software by using user subroutines, is only one of several similar ones, which shows the complexity of simulating discrete cracking in wooden boards with knots.

Our main research aim is to use this simulation tool in the development of new wood composites by making the material wood more predictable and thus more interesting for engineering applications. As the simulation of larger structures of wood-based products, where all inhomogeneities are modeled in high detail, might be not feasible in the near future, we developed a framework for sensitivity analysis and robust design optimization of structures made out of wood-based products [14], which is based on a random material model for both stiffness and strength properties of individual laminations. There, the varying material properties are condensed into so-called stiffness and strength profiles, where the presented numerical simulation tool for wooden boards with knots will vastly improve the quality of latter profiles.

First applications of such an approach showed very promising results. For example in [26], we used such randomly assigned strength profiles in the simulation of cross-laminated timber plates and could show that it is not just possible to correctly predict load capacities themselves but also their statistical variation, which were confirmed by experiments. In another application [27], stiffness profiles are used in a metamodel assisted optimization of glued laminated timber systems by reordering laminations using metaheuristic algorithms. This allows the optimized assignment of a batch of laminations to a set of GLT beams, such that an optimized load-bearing behavior is achieved.

Such simulations and developments should serve as basis for improved design concepts, the development of new and improvement of existing wood-based products, and could, finally, raise confidence in wood to a level where it should be.

REFERENCES

[1] M. Lukacevic, J. Füssl and R. Lampert, "Failure mechanisms of clear wood identified at wood cell level by an approach based on the extended finite element method," *Engineering Fracture Mechanics,* vol. 144, pp. 158-175, 2015.

[2] M. Lukacevic and J. Füssl, "Application of a multisurface discrete crack model for clear wood taking into account the inherent microstructural characteristics of wood cells," *Holzforschung,* vol. 70, pp. 845-853, 2016.

[3] M. Lukacevic, W. Lederer and J. Füssl, "A microstructure-based multisurface failure criterion for the description of brittle and ductile failure mechanisms of clear-wood," *Engineering Fracture Mechanics,* vol. 176, pp. 83-99, 5 2017.

[4] C. Hackspiel, K. Borst and M. Lukacevic, "A numerical simulation tool for wood grading model development," *Wood Science and Technology,* vol. 48, pp. 633-649, 2014.

[5] C. Hackspiel, K. Borst and M. Lukacevic, "A numerical simulation tool for wood grading: model validation and parameter studies," vol. 48, pp. 651-669, 2014.

[6] M. Lukacevic and J. Füssl, "Numerical simulation tool for wooden boards with a physically based approach to identify structural failure," *European Journal of Wood and Wood Products,* vol. 72, pp. 497-508, 2014.

[7] M. Lukacevic, J. Füssl, M. Griessner and J. Eberhardsteiner, "Performance assessment of a numerical simulation tool for wooden boards with knots by means of full-field deformation measurements," *Strain,* vol. 50, pp. 301-317, 2014.

[8] J. Ehlbeck, F. Colling and R. Görlacher, "Einfluss keilgezinkter Lamellen auf die Biegefestigkeit von Brettschichtholzträgern. Eingangsdaten für das Rechenmodell [Influence of finger-joints on the bending strength of GLT beams. Input data for the numerical model; Published in german]," *Holz als Roh- und Werkstoff,* vol. 43, pp. 369-373, 1985.

[9] O. Ditlevsen and B. Källsner, "Statistical series system effects on bending strength of timberbeams," in *Reliability and Optimization of Structural Systems*, 2004.

[10] C.-J. Johansson, "Grading of Timber with Respect to Mechanical properties," in *Timber Engineering,*

S. Thelandersson and H. J. Larsen, Eds., Chichester, John Wiley & Sons, 2003, pp. 23-43.

[11] R. Brandner and G. Schickhofer, "Glued laminated timber in bending: new aspects concerning modelling," *Wood Science and Technology,* vol. 42, pp. 401-425, 2008.

[12] M. Frese and H. J. Blaß, "Bending strength of spruce glulam," *European Journal of Wood and Wood Products,* vol. 67, no. 3, pp. 277-286, 2009.

[13] D. A. Garcia and M. B. Rosales, "Deflections in sawn timber beams with stochastic properties," *European Journal of Wood and Wood Products,* pp. 1-17, 2016.

[14] G. Kandler, M. Lukacevic, J. Füssl, C. Zechmeister and S. Wolff, "Stochastic engineering framework for timber structural elements," *Construction and Building Materials,* 2018.

[15] G. Kandler, M. Lukacevic and J. Füssl, "An algorithm for the geometric reconstruction of knots within timber boards based on fibre angle measurements," *Construction and Building Materials,* vol. 124, pp. 945-960, 2016.

[16] M. Lukacevic, J. Füssl and J. Eberhardsteiner, "Discussion of common and new indicating properties for the strength grading of wooden boards," *Wood Science and Technology,* vol. 49, pp. 551-576, 2015.

[17] W. Lederer, T. K. Bader, L. Muszynski and J. Eberhardsteiner, "Exploring a Multi-Modal Experimental Approach to Investigation of Local Embedment Behavior of Wood under Steel Dowels," *Strain,* vol. 52, pp. 531-547, 2016.

[18] L. Daudeville, "Fracture in spruce: experiment and numerical analysis by linear and non linear fracture mechanics," *Holz als Roh- und Werkstoff,* vol. 57, pp. 425-432, 1999.

[19] J. Nyström, "Automatic measurement of fiber orientation in softwoods by using the tracheid effect," *Computers and Electronics in Agriculture,* vol. 41, pp. 91-99, 2003.

[20] J. Zhou und J. Shen, „Ellipse detection and phase demodulation for wood grain orientation measurement based on the tracheid effect," *Optics and Lasers in Engineering,* Bd. 39, pp. 73-89, 2003.

[21] C. Hu, C. Tanaka and T. Ohtani, "On-line determination of the grain angle using ellipse analysis of the laser light scattering pattern image," *Journal of Wood Science,* vol. 50, pp. 321-326, 2004.

[22] A. Olsson and J. Oscarsson, "Three dimensional fibre orientation models for wood based on laser scanning utilizing the tracheid effect," in *Proceedings of the 2014 World Conference on Timber Engineering (WCTE), Quebec City, Canada,* 2014.

[23] L. Ingber, "Adaptive Simulated Annealing," *Intelligent Systems Reference Library,* vol. 35, pp. 33-62, 2012.

[24] C. Foley, "A three-dimensional paradigm of fiber orientation in timber," *Wood Science and Technology,* vol. 35, pp. 453-465, 2001.

[25] K. Hofstetter, C. Hellmich and J. Eberhardsteiner, "Development and experimental validation of a continuum micromechanics model for the elasticity of wood," *European Journal of Mechanics A/Solids,* vol. 24, pp. 1030-1053, 2005.

[26] M. Li, J. Füssl, M. Lukacevic, C. M. Martin and J. Eberhardsteiner, "Bending strength predictions of cross-laminated timber plates subjected to concentrated loading using 3D finite-element-based limit analysis approaches," *Composite Structures,* 2018.

[27] S. Pech, G. Kandler, M. Lukacevic und J. Füssl, „Metamodel assisted optimization of glued laminated timber systems by reordering laminations using metaheuristic algorithms," 2018.

[28] M. Li, J. Füssl, M. Lukacevic, J. Eberhardsteiner and C. M. Martin, "Strength predictions of clear wood at multiple scales using numerical limit analysis approaches," *Computers & Structures,* vol. 196, pp. 200-216, 2018.